Spin-Entangled Currents Created by a Triple Quantum Dot

Daniel S. Saraga and Daniel Loss

Department of Physics and Astronomy, University of Basel, Klingelbergstrasse 82, CH-4056 Basel, Switzerland

(Received 27 May 2002; published 24 April 2003)

We propose a simple setup of three coupled quantum dots in the Coulomb blockade regime as a source for spatially separated currents of spin-entangled electrons. The entanglement originates from the singlet ground state of a quantum dot with an even number of electrons. To preserve the entanglement of the electron pair during its extraction to the drain leads, the electrons are transported through secondary dots. This prevents one-electron transport by energy mismatch, while joint transport is resonantly enhanced by conservation of the total two-electron energy.

DOI: 10.1103/PhysRevLett.90.166803 PACS numbers: 73.63.–b, 03.65.Ud, 85.35.Be

The creation of entangled particles is a crucial problem as entanglement is a prerequisite for quantum computation and communication [1]. While various quantum information processing schemes have been successfully demonstrated with entangled photons [2], similar achievements are still missing for massive particles such as electrons. Hence there has been a number of theoretical proposals for a solid-state *entangler*—a device creating two entangled particles and allowing their separation and extraction into two distinct channels for further processing.

Recent proposals involve the extraction of entangled Cooper pairs from a superconductor in contact with quantum dots [3], normal or ferromagnetic conductors [4,5], and carbon nanotubes [6,7]. In another scheme, the entanglement arises from interference effects in a quantum dot in the cotunneling regime and requires special nondegenerate leads of narrow energy width [8]. A generic entangler based on interferometry and which-way detection was proposed in Ref. [9]. In this Letter, we propose an entangler based on a triple quantum dot setup. The entanglement originates from the singlet state of a pair of electrons in one quantum dot, while its transport relies on energy filtering by secondary dots. Our proposal is based on existing technology [10] and on realistic parameter values typical of quantum dot experiments.

Setup.—Figure 1 describes the proposed entangler. It is composed of three coupled lateral quantum dots (D_C, D_L, and D_R) in the Coulomb blockade regime, each of them coupled to a Fermi liquid lead l_C, l_L, and l_R. When two excess electrons are present in D_C, we can assume [11] that their ground state is the spin-singlet state, which is the (anti)symmetric superposition of their (spin) wave functions. The aim of the entangler is to extract the singlet from D_C, by transporting one electron into the neighboring dot D_L and the other one into D_R, and finally transport them into the drain leads l_L and l_R without loss of entanglement. This creates two currents of pairwise spin-entangled electrons that are spatially separated.

To preserve the entanglement of the electrons until they are in the drain leads, one must avoid the individual transport of one electron, as this would allow the arrival of a new electron in D_C which could destroy the existing entanglement by forming a new singlet with the remaining electron. To suppress one-electron transport, we arrange the dots to have a large difference between the energy levels of D_L and D_C compensated by the energy difference between D_R and D_C. This way the joint transport of both electrons to each neighboring dot conserves energy and is therefore enhanced by resonance, while the off-resonant transport of one electron is suppressed by the energy difference.

The number of electrons participating in the transport is controlled via Coulomb blockade [12], where N excess electrons in dot D_i ($i = C, L, R$) create a large electrostatic Coulomb charging energy $U_i(N)$. The energy of the Nth electron is then $E_i(N) = U_i(N) - U_i(N-1) + \epsilon_i(N)$, where $\epsilon_i(N)$ is the lowest single-particle energy available for the Nth electron. We consider the electrons to be independent and neglect further effects such as

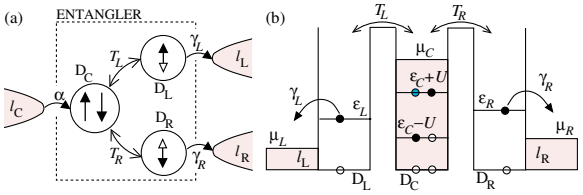

FIG. 1 (color online). (a) Setup of the triple quantum dot entangler. Three leads l_i ($i = C, L, R$) at chemical potential μ_i are coupled to three quantum dots D_i in the Coulomb blockade regime. Each dot contains an even number of electrons and can accept only zero, one (D_L and D_R), and two (D_C) excess electrons. A spin singlet is formed in D_C when two electrons tunnel incoherently, each with a rate α, from the source lead l_C into D_C. Each of the electrons can subsequently tunnel coherently to D_L and D_R with tunneling amplitudes T_L and T_R. Finally, the electrons tunnel out (with rates γ_L and γ_R) to the drain leads l_L and l_R, creating two currents of entangled electrons. (b) Energy level diagram, for *each* electron. Unentangled currents, which arise from one-electron transport, are suppressed by the energy differences $\epsilon_{L,R} - \epsilon_C \pm U$. The joint transport of both electrons is favored by a resonance in the total two-electron energy: $\epsilon_L + \epsilon_R \simeq 2\epsilon_C$.

interdot charging energy or exchange Coulomb interaction. Assuming a shell filling of each dot [12], we disregard all but the excess electrons in each dot. The ground state in D_C with two excess electrons is the spin singlet $\uparrow\downarrow - \downarrow\uparrow$, where both electrons have the same orbital energy $\epsilon_C = \epsilon_C(1) = \epsilon_C(2)$. For convenience of notation, we set the gate voltage of each dot so that $U_j(0) = U_j(1)$, $j = L, R$ and $U_C(0) = U_C(2) = 0$, which gives a negative charging energy for one electron: $U_C(1) = -U$. We define the zero energy as the total energy of the three empty dots.

The chemical potentials μ_i in the leads are tuned to allow only zero or one excess electron in D_j, $j = L, R$, and zero, one, or two electrons in D_C. It is crucial that only the ground states of the electronic levels in the dots participate in the transport. To avoid resonance with excited levels, the energy level spacings in the dots must be larger than the Coulomb charging energies: $\Delta\epsilon_i > U_i$. Excited states with energy E_i^* could participate in the transport through cotunneling events [12], which are second-order transport processes involving "virtual states" in the dots. We neglect such channels, as they are suppressed by factors of the order of $\alpha/(E_i^* - \mu_i) \simeq \alpha/(U_i - \mu_i) \ll 1$. We need low temperatures T so that thermal fluctuations cannot allow three electrons in D_C or populate excited levels, which could also create a current in the reverse direction ($l_j \to D_j$, $D_C \to l_C$). Taking $k_B T \ll |\mu_i - E_i(0, 1, 2, 3)|$, we can neglect temperature effects and set $T = 0$ for simplicity.

The quantum states of the entangler are given by combining the different numbers of electrons allowed in each dot. 0 describes the situation where all the dots are empty; L, R, or C corresponds to one electron in D_L, D_R, or D_C, while CC denotes the singlet state created by two electrons in D_C. Thus, the eight states, shown in Fig. 2 with their transitions, form the basis set $\mathcal{B} = \{0, C, CC, LC, CR, LR, L, R\}$. This description in terms of the individual levels of each isolated dot requires that the tunneling matrix elements T_L and T_R (considered to be real) connecting the dots are small and do not mix the levels in different dots, i.e., $T_L, T_R \ll \Delta\epsilon_i$.

The coherent evolution between the dots is described by a Hamiltonian matrix $H_{k,k'}$, $k, k' \in \mathcal{B}$. The diagonal elements contain the energies $E_0 = 0$, $E_C = \epsilon_C - U$, $E_{CC} = 2\epsilon_C$, $E_{LC} = \epsilon_L + \epsilon_C - U$, $E_{CR} = \epsilon_R + \epsilon_C - U$, $E_{LR} = \epsilon_L + \epsilon_R$, $E_L = \epsilon_L$, $E_R = \epsilon_R$, while the off-diagonal elements describe the coherent oscillations of one electron between D_C and D_L or D_R: $H_{C,L} = H_{CR,LR} = T_L$, $H_{C,R} = H_{LC,LR} = T_R$, $H_{CC,LC} = T_L\sqrt{2}$ and $H_{CC,CR} = T_R\sqrt{2}$. The $\sqrt{2}$ factor comes from the identical orbital states in CC.

We describe the incoherent transport from/to the leads as sequential tunneling (lowest order in $\alpha, \gamma_L, \gamma_R$), and treat it with a master equation for the reduced density matrix ρ of the entangler. The diagonal elements ρ_k, $k \in \mathcal{B}$ are the occupation probabilities of the state k, with normalization $\sum_k \rho_k = 1$. The off-diagonal elements $\rho_{k,k'}$ contain the coherent superposition of k and k'. We write the master equation [13] as $d\rho/dt = -i[H, \rho] - M$, where M describes the incoherent transport connecting a state k to another state k' with a rate $W(k', k) \in \{\alpha, \gamma_L, \gamma_R\}$. For the diagonal elements, this results in the population equation $M_k = -\rho_k \sum_{k'} W(k', k) + \sum_{k'} W(k, k')\rho_{k'}$, while the off-diagonal elements are damped by the incoherent transitions out of each of the two corresponding states: $M_{k,k'} = -\frac{1}{2}\rho_{k,k'} \times \sum_{k'' \neq k,k'} W(k'', k) + W(k'', k')$. Out of the 64 elements of ρ, only 26 are coupled to the relevant diagonal elements. Arranging them in a real vector $\vec{V}$, one can rewrite the master equation as a homogeneous first-order differential equation given by a 26×26 matrix $\mathcal{A}$: $d\vec{V}/dt = \mathcal{A}\vec{V}$. Its stationary solution is the eigenvector corresponding to the zero eigenvalue of $\mathcal{A}$. It can be found symbolically by a mathematical software (MAPLE) and defines the stationary populations $P_k = \rho_k^0$ of the different states k of the entangler.

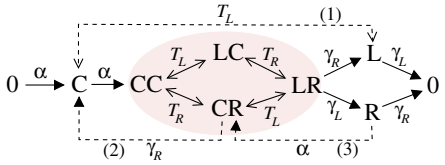

FIG. 2 (color online). The entangler states $\{0, C, CC, LC, CR, LR, L, R\}$ and their transitions. Double arrows indicate coherent oscillations of one electron between two dots with overlap matrix element T_L and T_R (in the shaded area). Single arrows indicate incoherent tunneling from (α) or to (γ_L and γ_R) the leads. The dashed lines indicate the three types of transitions that must be avoided to ensure the joint transport of the singlet pair CC to the leads (see text; for clarity we do not show the transitions obtained by replacing L by R).

Results.—We define currents by multiplying the different P_k by the relevant rates: γ_L and γ_R for the output current and α for the input current. We plot in Fig. 3(a) the current in the left (I_L) and right (I_R) drain leads, as a function of $\delta\epsilon_L = \epsilon_L - \epsilon_C$. We consider a symmetric setup with $\gamma = \gamma_L = \gamma_R$ and $T_0 = T_L = T_R$ and fix the energy in the right dot, $\epsilon_R = \epsilon_C$, which implies that I_R is almost constant. The middle peak of I_L at $\delta\epsilon_L = 0$ is the desired two-electron resonance defined by $E_{CC} = E_{LR}$. The other two peaks are due to one-electron resonances: between CC and LC when $\delta\epsilon_L = U$ and between C and L when $\delta\epsilon_L = -U$.

Next we consider the total current leaving the device, defined by $I = I_L + I_R$. The central goal is to prove that at resonance ($\delta\epsilon_L = 0$) it is dominated by the contribution from entangled electron pairs (spin singlets), i.e., $I \simeq I_E$; see below and Fig. 3(a). This contribution is a coherent "second-order" transport process where one partner leaves into lead l_L and the other one into lead l_R. For this proof we need to consider also the contribution from unentangled pairs. The latter can occur only from single-particle transport with no coherence between the outgoing electrons. Such incoherent "first-order"

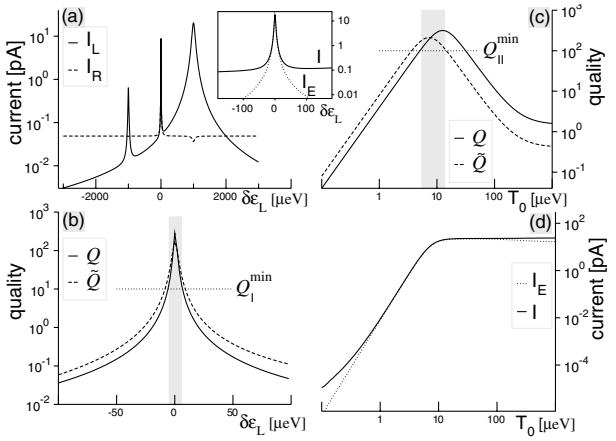

FIG. 3. Currents and qualities of the entangler, with $\alpha = 0.1$, $\gamma = 1$, $T_0 = 10$, $U = 1000$ in μeV. (a) Total current in the left (I_L) and right (I_R) leads. The symmetric current $I_L = I_R$ at the central peak is a signature of the two-electron resonance, where the current is dominated by the entangled current I_E. The peaks at $\delta\epsilon_L = \pm U$ are resonances for the transport of one electron. The inset shows I_E and the total current $I = I_L + I_R$, around $\delta\epsilon_L = 0$. (b) Qualities Q and $\tilde{Q}$ around the resonance at $\delta\epsilon_L = 0$, where the entangled current dominates. The width of the resonance defined by $Q, \tilde{Q} > Q_{\rm I}^{\rm min} = 10$ is $|\delta\epsilon_L| < 6$ μeV, as given by Eq. (7) (gray region). (c) Q and $\tilde{Q}$ vs the tunneling amplitude T_0, at resonance ($\delta\epsilon_L = 0$). In gray, the region where the quality of the entangler is $Q, \tilde{Q} > Q_{\rm II}^{\rm min} = 100$; see Eq. (8). (d) At resonance, the entangled current $I_E \simeq I$ saturates to $\simeq e\alpha = 20$ pA when $T_0 \gg 5$ μeV.

processes can occur only in the following three ways; see Fig. 2.

(1) An electron tunnels from D_C to D_L and then out to l_L before a second electron has tunneled into D_C and formed a singlet. As the stationary solution contains no information on the history of the electrons, we must compare currents obtained in the following two cases. (i) We switch off the undesired channel by setting $T_L = T_R = 0$ between C, L, and R, while keeping the tunneling between CC, CR, LC, and LR. This redefines the populations P_k. Now we can define the stationary *entangled current* by $I_E = e\gamma_L(P_{LR} + P_L) + e\gamma_R(P_{LR} + P_R)$; see the central sequence in Fig. 2. (ii) We keep the undesired channel, while switching off the tunneling involving CC and LR. This defines the populations $\tilde{P}_k$ and creates a current $e\gamma_L(\tilde{P}_L + \tilde{P}_{LC}) + e\gamma_R(\tilde{P}_R + \tilde{P}_{CR})$ which carries no entangled pairs. This leakage current is small, as it is an off-resonant process suppressed by the energy mismatch $\epsilon_{L,R} - \epsilon_C + U$ between the initial state C and the final states L, R. Defining the *entangler quality* by $\tilde{Q} = \min\{P_L/\tilde{P}_L, P_{LR}/\tilde{P}_{LC}, P_R/\tilde{P}_R, P_{LR}/\tilde{P}_{CR}\}$, the leakage current is negligible when $\tilde{Q} \gg 1$.

(2) An electron tunnels out from D_L to l_L while the second electron is still in D_C. This creates a current $e\gamma_L P_{LC}$ which might contain no entanglement, as the remaining electron can form a new singlet with a new electron coming from l_C. This current is suppressed by the energy mismatch $\epsilon_L - \epsilon_C - U$ between the states CC and LC. We define a second entangler quality by $Q = \min\{P_{LR}/P_{CR}, P_{LR}/P_{LC}\}$, which ensures that the entangled current I_E is dominant if $Q \gg 1$.

(3) After the joint transport of the two electrons into the state LR and the tunneling of one electron into l_L, a new electron tunnels into D_C before the remaining electron in D_R has tunneled out to l_R. The new electron can then form a new singlet with the remaining electron, therefore destroying the entanglement that existed with the electron which has moved to the lead l_L. To suppress this channel, we need $\alpha \ll \gamma_L, \gamma_R$. For simplicity, we set $\alpha = 0$ for transitions from L and R when calculating the probabilities P_k (although we keep α nonzero for $\tilde{P}_k$).

Now we compare I with I_E by solving the master equation numerically. At the resonance $\delta\epsilon_L = 0$, we find that $I \simeq I_E$ within a few percent for a realistic set of parameters; see the inset in Figs. 3(a) and 3(d). Hence, *at resonance the total current I consists essentially of entangled electron pairs.* Next we derive analytical conditions for the range of validity of $I \simeq I_E$, with the help of the entangler qualities Q and $\tilde{Q}$ defined above. The exact analytical expressions for P_k are extremely lengthy and cannot be written in a compact form. From a heuristic analysis involving first- and second-order perturbation calculations, we find that the second-order transition rate (corresponding to the transport of entangled electrons) dominates if $\alpha \ll \gamma \ll T_0 \ll U, |U \pm \delta\epsilon_L|$ [14]. Hence we expand both the numerator and denominator of the expressions for P_k in the lowest nontrivial order in α, γ, T_0. We distinguish two cases:

(I) nonresonant ($|\delta\epsilon_L| > T_0$):

$$P_L = P_R = P_{LR} \simeq \frac{2T_0^4(2U - \delta\epsilon_L)^2}{\delta\epsilon_L^2 U^2 (U - \delta\epsilon_L)^2}, \tag{1}$$

$$P_{CR} \simeq \frac{2T_0^2}{U^2}, \qquad P_{LC} \simeq \frac{2T_0^2}{(U - \delta\epsilon_L)^2}, \tag{2}$$

$$\tilde{P}_R \simeq \frac{T_0^2}{U^2}, \qquad \tilde{P}_L \simeq \frac{T_0^2}{(U + \delta\epsilon_L)^2}, \tag{3}$$

(II) resonant ($\delta\epsilon_L = 0$):

$$P_L = P_R = P_{LR} \simeq \frac{8\alpha T_0^4}{\alpha\gamma^2 U^2 + 32\gamma T_0^4}, \tag{4}$$

$$P_{CR} = P_{LC} \simeq \frac{2\alpha T_0^2(\gamma^2 U^2 + 40T_0^4)}{U^2(\alpha\gamma^2 U^2 + 32\gamma T_0^4)}, \tag{5}$$

$$\tilde{P}_R = \tilde{P}_L \simeq \frac{\alpha\gamma T_0^2}{\alpha\gamma U^2 + 2\gamma^2 T_0^2}, \tag{6}$$

and $\tilde{P}_{CR} = \tilde{P}_R\alpha/\gamma$, $\tilde{P}_{LC} = \tilde{P}_L\alpha/\gamma$.

These two cases are sufficient for an analytical discussion of the entangler qualities, as the approximate expressions (1)–(6) reproduce accurately the *exact*

numerical results presented in Fig. 3. As shown in Fig. 3(b), the entangler qualities Q and $\tilde{Q}$ reach a maximum at $\delta\epsilon_L = 0$, which is due to the resonance in the coherent oscillations between CC and LR. We define now the quantities $Q_{\rm I}$ and $\tilde{Q}_{\rm I}$ as the approximations of the qualities Q and $\tilde{Q}$ obtained with Eqs. (1)–(3). $Q_{\rm I}$ and $\tilde{Q}_{\rm I}$, which grow as $(\delta\epsilon_L)^{-2}$, give a correct estimate of the width $\overline{\delta\epsilon}_L$ of the resonance around $\delta\epsilon_L = 0$. Introducing the condition $Q_{\rm I}, \tilde{Q}_{\rm I} > Q_{\rm I}^{\rm min}$, we get

$$|\delta\epsilon_L| < \overline{\delta\epsilon}_L = 2T_0/\sqrt{Q_{\rm I}^{\rm min}}. \tag{7}$$

Note that such proportionality of the width to the tunneling matrix element is also found in the Rabi formula for a two-level system. Similarly, we define $Q_{\rm II}$ and $\tilde{Q}_{\rm II}$ with Eqs. (4)–(6); these approximate ratios accurately reproduce the height of the resonance peak at $\delta\epsilon_L = 0$. Introducing the condition $Q_{\rm II}, \tilde{Q}_{\rm II} > Q_{\rm II}^{\rm min}$, we find

$$\gamma\sqrt{Q_{\rm II}^{\rm min}/8} < T_0 < U\sqrt{\alpha/4\gamma Q_{\rm II}^{\rm min}} \tag{8}$$

as illustated in Fig. 3(c). We note that Eqs. (7) and (8) can be approximately derived using the rates obtained from a perturbative calculation [14].

Quantities which are experimentally accessible are the total currents in the left and right leads, I_L and I_R. We see in Fig. 3(a) that the current is asymmetric away from the two-electron resonance: $I_L \neq I_R$. On the other hand, it is symmetric around $\delta\epsilon_L = 0$, as the two electrons are transported jointly from the central dot D_C to l_l and l_R. Hence one can find the resonance—and the regime where the entangler is most efficient—by varying ϵ_L via the gate voltage of D_L until $I_L = I_R$ [15]. Finally, Eq. (4) gives $P_{LR} \simeq \alpha/4\gamma$ for $T_0^4 \gg U^2\gamma\alpha/32$, which yields $I_E \simeq I_{\rm max} = e\alpha$, as illustrated in Fig. 3(d). In this case the bottleneck is the tunneling from l_C. Note that in order to be able to reach $I_{\rm max}$ within regime (8), one also needs $U > Q_{\rm II}^{\rm min}\gamma\sqrt{\gamma/2\alpha}$.

Discussion.—Setting the qualities of the entangler to $Q_{\rm II}^{\rm min} = 100$, $Q_{\rm I}^{\rm min} = 10$, and $\gamma = 10\alpha$, we need approximately $35\alpha < T_0 < U/60$ and $U > 2200\alpha$. The first condition is easily met as α and T_0 can be varied via the voltages defining the barriers [16]. For the second condition, we take a realistic value for the current, $I_L \simeq$ 10 pA [16], yielding $\alpha > 0.1$ μeV $\Rightarrow U > 0.3$ meV. To get a finite width $\overline{\delta\epsilon}_L \simeq 6$ μeV, we take $U \simeq 1$ meV, which is within reported values [12,16]. To obtain an even better quality ($Q_{\rm II}^{\rm min} = 1000$, $\gamma = 100\alpha$), one needs to increase the ratio U/α. One possible issue is the single-particle energy spacing $\Delta\epsilon_i$, which is usually smaller than or equal to the charging energy. However, as $\Delta\epsilon_i \sim 1/L^2$ in a box of size L, while $U \sim 1/L$, one should be able to reach $\Delta\epsilon_i > U$ by decreasing the dot size. Alternatively, one can use vertical quantum dots, which have large energy level spacings [12], or use one carbon nanotube with two bendings (which defines three regions behaving like quantum dots).

A current $I_{\rm max} \simeq 20$ pA corresponds to the delivery of a spin-entangled pair every $t_{\rm p} \simeq 2/\alpha \simeq 15$ ns. The average separation between two entangled electrons is approximately $t_{\rm e} \simeq 1/U \simeq 0.6$ ps $\ll t_{\rm p}$, with a maximal separation of $t_{\rm m} \simeq 1/\gamma \simeq 0.6$ ns. Note that both $t_{\rm e}$ and $t_{\rm m}$ are below reported spin decoherence times of 100 ns [17]. This would allow noise measurements using a beam splitter, where an enhancement in the two-terminal noise is a signature of singlet states compared to the noise of uncorrelated electrons [18]. We emphasize that such an experiment requires electrons with the same orbital energy, which can be achieved here for $\epsilon_L = \epsilon_R = \epsilon_C$. One could also carry out a measurement of Bell inequalities by measuring the spin of the electron in each lead with the help of a spin filter based on a quantum dot [19].

We thank H. A. Engel, P. Recher, C. Egues, and G. Burkard for useful discussions. Financial support from NCCR Nanoscale Science, the Swiss NSF, U.S. DARPA, and ARO is gratefully acknowledged.

[1] C. H. Bennett and D. P. DiVincenzo, Nature (London) **404**, 247 (2000).
[2] W. Tittel and G. Weihs, Quantum Inf. Comput. **1**, 3 (2001), and references therein.
[3] P. Recher, E. V. Sukhorukov, and D. Loss, Phys. Rev. B **63**, 165314 (2001).
[4] G. B. Lesovik, T. Martin, and G. Blatter, Eur. Phys. J. B **24**, 287 (2001).
[5] R. Mélin, cond-mat/0105073; G. Falci, D. Feinberg, and F. W. J. Hekking, Europhys. Lett. **54**, 255 (2001).
[6] P. Recher and D. Loss, Phys. Rev. B **65**, 165327 (2002).
[7] C. Bena, S. Vishveshwara, L. Balents, and M. P. A. Fisher, Phys. Rev. Lett. **89**, 037901 (2002).
[8] W. D. Oliver, F. Yamaguchi, and Y. Yamamoto, Phys. Rev. Lett. **88**, 037901 (2002).
[9] S. Bose and D. Home, Phys. Rev. Lett. **88**, 050401 (2002).
[10] F. R. Waugh *et al.*, Phys. Rev. Lett. **75**, 705 (1995).
[11] S. Tarucha *et al.*, Phys. Rev. Lett. **84**, 2485 (2000).
[12] L. P. Kouwenhoven *et al.*, in *Mesoscopic Electron Transport*, NATO ASI, Ser. E, Vol. 345 (Kluwer, Dordrecht, 1997).
[13] K. Blum, *Density Matrix Theory and Applications* (Plenum, New York, 1996).
[14] The condition is $W_1 \ll \alpha \ll W_2$, where W_1 are the first-order rates corresponding to the processes (1) and (2), W_2 are the second-order rates corresponding to $CC \rightarrow LC, CR \rightarrow LR$, and we consider a Lorentzian broadening of the final states due to the coupling to the leads.
[15] With an asymmetry of 10% ($\gamma_L = 0.9\gamma_R, T_L = 1.1T_R$), the left and right currents differ by 10% at resonance, and the entangler qualities $Q, \tilde{Q}$ are reduced by 15%.
[16] T. H. Oosterkamp *et al.*, Nature (London) **395**, 873 (1998); T. Fujisawa *et al.*, Science **282**, 932 (1998).
[17] J. M. Kikkawa and D. D. Awschalom, Phys. Rev. Lett. **80**, 4313 (1998).
[18] G. Burkard, D. Loss, and E. V. Sukhorukov, Phys. Rev. B **61**, R16 303 (2000).
[19] P. Recher, E. V. Sukhorukov, and D. Loss, Phys. Rev. Lett. **85**, 1962 (2000).